CRAMER RAO BOUNDS ON DIRECTION ESTIMATES FOR CLOSELY SPACED EMITTERS IN MULTI-DIMENSIONAL APPLICATIONS

Jack Jachner and Harry Lee

Atlantic Aerospace Electronics Corp.
470 Totten Pond Rd., Waltham, MA 02154, USA

ABSTRACT

The main results of this paper are characterizations of the Cramer-Rao (CR) bound on the variance of direction estimates for closely-spaced emitters in multiple parameter (multi-D) scenarios. Specifically, simple analytic expressions for the CR bound are presented for co-linear emitter configurations, which show the bound to be very sensitive to the maximum spacing between emitters ($\delta\omega$). Results also are cited for CR bound sensitivity to $\delta\omega$ for emitter configurations in which the emitters are not co-linear. The latter results exhibit greatly reduced sensitivity to the direction separation factor $\delta\omega$. Thus the results show that *degeneracies are present in multi-D parameter estimation scenarios that are not present in 1-D scenarios.* Specifically emitter resolution and direction estimation can be expected to be much more challenging for some emitter configuration than for others. The case of co-linear emitters appears to be a particularly stressful one.

1. INTRODUCTION

The Cramer-Rao (CR) bound on the variance of direction estimates provides a useful benchmark for assessing estimation accuracy of direction-finding algorithms. Evaluation of the CR bound generally requires inverting the applicable Fisher Information matrix, leading to expressions in terms of matrix inverses [1],[2]. For closely-spaced emitters, simple analytic expressions for the CR bound applicable to single parameter (1-D) direction finding problems have been obtained [3]. This paper extends the latter result to example multi-dimensional (multi-D) direction finding scenarios, and shows that behavior of the bound is strongly dependent upon the emitter configuration.

2. PROBLEM ASSUMPTIONS

We utilize the data model of [1]. Specifically assume that parameter vectors $\vec{\omega}_1 \cdots \vec{\omega}_n$ are to be estimated from N data vectors ("snapshots") of the form

$$\vec{y}(t) = A \cdot \vec{x}(t) + \vec{e}(t) \qquad t = 1 \cdots N \qquad (1)$$

$\vec{y}(t)$ is a noisy (complex) $m \times 1$ vector observed at sample index t. A is a constant $m \times n$ matrix of n signal vectors having the special form

$$A \triangleq [\vec{a}(\vec{\omega}_1), \cdots \vec{a}(\vec{\omega}_n)] \qquad (2)$$

This research was funded in part by the U.S. Navy - Office of Naval Research under Grant No. N00014-91-J-1628

$\vec{a}(\vec{\omega})$ is a known generic signal vector for parameter vector $\vec{\omega} = [\omega_1, \cdots \omega_d]^T$. $\vec{x}(t)$ is an unknown $n \times 1$ vector of complex amplitudes which can change with index t. $\vec{e}(t)$ is an $m \times 1$ vector of additive complex noise at sample index t.

Let superscripts ^{T} and * denote the transpose and the conjugate transpose respectively.

Paralleling Reference [1], assume that $m > n$, that the elements of $\vec{a}(\omega)$ are bounded and possess derivatives of all orders, that the sequence of vectors $\vec{x}(t)$ $t = 1 \cdots N$ is fixed for all realizations of the data sequence $\vec{y}(t)$, that the matrix

$$P \triangleq \frac{1}{N} \sum_{t=1}^{N} \vec{x}(t)\vec{x}(t)^* \qquad (3)$$

is positive definite, and that the vector $\vec{e}(t)$ varies randomly across the ensemble of data vectors $\vec{y}(t)$. Specifically the $\vec{e}(t)$ are samples of a zero-mean, uncorrelated complex Gaussian random process with variance σ. The data model (1)-(3) often is designated as the Conditional Model [1], [3].

3. CR BOUND EXPRESSION

The CR bound applicable to the parameter vectors $\vec{\omega}_1 \cdots \vec{\omega}_n$ takes the following form. If $\hat{\omega}_{ji}$ is an unbiased estimate of the j^{th} element of $\vec{\omega}_i$, $(j = 1 \cdots d, i = 1 \cdots n)$, then

$$\mathrm{Cov}\left\{\vec{\hat{\omega}}\right\} = E\left\{\left(\vec{\hat{\omega}} - \vec{\omega}\right)\left(\vec{\hat{\omega}} - \vec{\omega}\right)^*\right\} \geq B_C \qquad (4)$$

where $E\{\,\}$ denotes expectation, $A \geq B$ means that the matrix $A - B$ is non-negative definite, and

$$\vec{\hat{\omega}} \triangleq [\hat{\omega}_{11} \cdots \hat{\omega}_{1n} \cdots \hat{\omega}_{d1} \cdots \hat{\omega}_{dn}]^T \qquad (5)$$

$$\vec{\omega} \triangleq E\left\{\vec{\hat{\omega}}\right\} \qquad (6)$$

B_C is the $nd \times nd$ submatrix of the inverse Fisher Information matrix corresponding to the suitably ordered elements of $\vec{\omega}_1 \cdots \vec{\omega}_n$.

In Reference [1], Stoica and Nehorai derive an expression for B_C^{-1} valid for one-dimensional parameter scenarios. Yau and Bresler extend the result to vector parameters $\vec{\omega}$ in Reference [2]. Straightforward re-arrangement of Equation (9) of [2] gives

$$B_C^{-1} = \frac{2N}{\sigma} \mathrm{Re}\left[H \odot P_+^T\right] \qquad (7)$$

0-7803-0532-9/92 $3.00

where $\odot$ denotes the Hadamard element-by-element matrix product, and

$$H \triangleq \Gamma^* \Gamma \tag{8}$$

$$\Gamma \triangleq [\vec{\gamma}_1(\vec{\omega}_1), \cdots \vec{\gamma}_1(\vec{\omega}_n), \cdots \vec{\gamma}_d(\vec{\omega}_1), \cdots \vec{\gamma}_d(\vec{\omega}_n)] \tag{9}$$

$$\vec{\gamma}_j(\vec{\omega}_i) \triangleq \left[I - A(A^*A)^{-1}A^*\right] \left[\frac{\partial}{\partial \zeta_j} \vec{a}(\vec{\zeta})\right]_{\vec{\zeta}=\vec{\omega}_i} \tag{10}$$

where $\vec{\zeta} = [\zeta_1 \cdots \zeta_d]^T$ and

$$P_+ \triangleq \begin{bmatrix} P & \cdots & P \\ \vdots & & \vdots \\ P & \cdots & P \end{bmatrix} \qquad (nd \times nd) \tag{11}$$

4. ANALYSIS APPROACH

The main results of this paper are obtained by identifying the dominant term for small parameter separations of (7) for selected multi-dimensional scenarios. Following Reference [3], we express $\vec{\omega}_i$ as follows

$$\vec{\omega}_i = \vec{\omega}_0 + \delta\omega \cdot \vec{q}_i \tag{12}$$

$i = 1 \cdots n$, where $\vec{\omega}_0$ is a nearby fixed reference vector, $\delta\omega$ is a variable real scalar parameter, and

$$\vec{q}_i = [q_{1i}, \cdots q_{di}]^T \tag{13}$$

$i = 1 \cdots n$ are constant normalized real parameter offset vectors. The $\vec{q}_i$ are normalized so that $\delta\omega$ measures the maximum separation $\|\vec{\omega}_k - \vec{\omega}_l\|$ between pairs of the parameter vectors $\vec{\omega}_1 \cdots \vec{\omega}_n$.

The analysis strategy is to examine the behavior of (7) as the scaling parameter $\delta\omega \rightarrow 0$, while the $\vec{q}_i$ are held constant.

5. CO-LINEAR EMITTERS IN MULTI-D

The first case that we address is that of estimating the multi-dimensional angle of arrival for *n co-linear emitters with arbitrary spacing.* To simplify the analysis, assume 1) that the spatial line of the emitters parallels the coordinate axis for the first angular variable, and 2) that the remaining angular variables are measured relative to the emitter line along orthogonal coordinate axes. That is, assume

$$\vec{\omega}_i = \vec{\omega}_0 + [\delta\omega\, q_i, 0, \cdots 0]^T \tag{14}$$

$i = 1 \cdots n$. (Note that this assumption does not constrain the sensor array. Specifically we are not assuming that the line of emitters coincides with a line of sensor array symmetry.)

Use of results presented in [3] (specifically Eqs (A.19), (A.2)-(A.6)), shows that as $\delta\omega \rightarrow 0$ the dominant terms of the columns of (9) are as follows:

$$\begin{aligned} \vec{\gamma}_1(\vec{\omega}_i) &= \delta\omega^{n-1} \frac{\phi'(q_i)}{n!} \vec{\chi} + \mathcal{O}(\delta\omega^n) \\ \vec{\gamma}_j(\vec{\omega}_i) &= \vec{\psi}_j + \mathcal{O}(\delta\omega) \end{aligned} \tag{15}$$

$i = 1 \cdots n$, $j = 2 \cdots d$, with the constant vectors

$$\begin{aligned} \vec{\chi} &\triangleq [I - \dot{A}(\dot{A}^*\dot{A})^{-1}\dot{A}^*]\, \vec{a}^{(n)}_{1\cdots 1} \\ \vec{\psi}_j &\triangleq [I - \dot{A}(\dot{A}^*\dot{A})^{-1}\dot{A}^*]\, \vec{a}^{(1)}_j \end{aligned} \tag{16}$$

where $\dot{A}$ is the constant matrix

$$\dot{A} \triangleq \left[\vec{a}(\vec{\omega}_0), \vec{a}^{(1)}_1, \cdots \vec{a}^{(n-1)}_{1\cdots 1}\right] \tag{17}$$

$$\vec{a}^{(k)}_{j_1 \cdots j_k} \triangleq \left[\frac{\partial}{\partial \zeta_{j_1}} \cdots \frac{\partial}{\partial \zeta_{j_k}} \vec{a}(\vec{\zeta})\right]_{\vec{\zeta}=\vec{\omega}_0} \tag{18}$$

and

$$\phi'(q_i) \triangleq \prod_{\substack{l=1 \\ l \neq i}}^{n} (q_i - q_l) \tag{19}$$

It can be shown that the $\vec{\chi}$, $\vec{\psi}_2 \cdots \vec{\psi}_d$ are non-zero and linearly independent if the columns of $\dot{A}$, $\vec{a}^{(n)}_{1\cdots 1}$, $\vec{a}^{(1)}_2, \cdots \vec{a}^{(1)}_d$ are linearly independent. Many sensor array geometries of interest satisfy this condition, and we assume it to be true in this analysis.

It follows from (15) that (7) can be expressed as

$$\begin{aligned} B_C^{-1} &= \frac{2N}{\sigma} \mathrm{Re}\left[(\Gamma^*\Gamma) \odot P_+^T\right] \\ &= \frac{2N}{\sigma} \Phi \left\{K + \mathcal{O}(\delta\omega)\right\} \Phi \end{aligned} \tag{20}$$

where

$$\Phi \triangleq \mathrm{Diag}\left[\delta\omega^{n-1} \frac{\phi'(q_1)}{n!}, \cdots \delta\omega^{n-1} \frac{\phi'(q_n)}{n!}, 1, \cdots 1\right] \tag{21}$$

$$K \triangleq \mathrm{Re}\begin{bmatrix} (\vec{\chi}^*\vec{\chi})P^T & (\vec{\chi}^*\vec{\psi}_1)P^T & \cdots & (\vec{\chi}^*\vec{\psi}_d)P^T \\ (\vec{\psi}_1^*\vec{\chi})P^T & (\vec{\psi}_1^*\vec{\psi}_1)P^T & \cdots & (\vec{\psi}_1^*\vec{\psi}_d)P^T \\ \vdots & \vdots & \ddots & \vdots \\ (\vec{\psi}_d^*\vec{\chi})P^T & (\vec{\psi}_d^*\vec{\psi}_1)P^T & \cdots & (\vec{\psi}_d^*\vec{\psi}_d)P^T \end{bmatrix} \tag{22}$$

It can be shown that the constant matrix K is positive definite if $\vec{\chi}$, $\vec{\psi}_2, \cdots \vec{\psi}_d$ are linearly independent. Therefore we have

$$B_C = \frac{\sigma}{2N} \Phi^{-1} \left\{K^{-1} + \mathcal{O}(\delta\omega)\right\} \Phi^{-1} \tag{23}$$

The following general form of the CR bound on each of the $\hat{\omega}_{ji}$ follows from (23) and the $\delta\omega$ dependence of Φ in (21):

$$\begin{aligned} \mathrm{Var}\{\hat{\omega}_{1i}\} &\geq \frac{1}{N \cdot \mathrm{SNR}_i} \frac{b_{1i}}{\delta\omega^{2(n-1)}} + \mathcal{O}(\delta\omega^{-2(n-1)+1}) \\ \mathrm{Var}\{\hat{\omega}_{ji}\} &\geq \frac{1}{N \cdot \mathrm{SNR}_i} b_{ji} + \mathcal{O}(\delta\omega) \end{aligned} \tag{24}$$

for $i = 1 \cdots n$, $j = 2 \cdots d$, where SNR_i denotes the signal-to-noise ratio for the i^{th} emitter

$$\mathrm{SNR}_i \triangleq (P)_{ii}/\sigma \tag{25}$$

$(\,)_{rs}$ denotes the r,s^{th} element of the referenced matrix and b_{1i}, b_{ji} are positive constants straightforwardly calculable from (23).

Eqs. (24) are important because they make explicit the small $\delta\omega$ behavior of the CR bound. Specifically as $\delta\omega \to 0$, the CR variance bound for the angular coordinate along the emitter line is asymptotically proportional to $1/\delta\omega^{2(n-1)}$; therefore the bound increases rapidly as $\delta\omega \to 0$. By contrast the bounds for angular coordinates perpendicular to this line are asymptotically constant. Thus the bound for any angular coordinate not perpendicular to the emitter line also is proportional to $1/\delta\omega^{2(n-1)}$.

5.1 Special Cases

More explicit expressions can be obtained if any of the following conditions are satisfied.

I P is real. (This includes the uncorrelated emitter case for which P is diagonal.)

II All inner products of vectors $\vec{\chi}$, $\vec{\psi}_2, \cdots \vec{\psi}_d$ are real. (This condition occurs automatically for arrays of omni-directional sensors with pair-wise sensor symmetry about the array center.)

III All vectors $\vec{\chi}$, $\vec{\psi}_2, \cdots \vec{\psi}_d$ are orthogonal. (This condition occurs for 2-D sensor arrays with the above symmetry if the number of emitters is even.)

If any of the above conditions is satisfied, then

$$K^{-1} = \begin{bmatrix} \alpha_{11}(\mathrm{Re}\left[P^T\right])^{-1} & \cdots & \alpha_{1d}(\mathrm{Re}\left[P^T\right])^{-1} \\ \vdots & & \vdots \\ \alpha_{d1}(\mathrm{Re}\left[P^T\right])^{-1} & \cdots & \alpha_{dd}(\mathrm{Re}\left[P^T\right])^{-1} \end{bmatrix} \quad (26)$$

where the α_{ji} are the real constant elements of

$$\begin{bmatrix} (\vec{\chi}^*\vec{\chi}) & \mathrm{Re}\left[\vec{\chi}^*\vec{\psi}_1\right] & \cdots & \mathrm{Re}\left[\vec{\chi}^*\vec{\psi}_d\right] \\ \mathrm{Re}\left[\vec{\psi}_1^*\vec{\chi}\right] & (\vec{\psi}_1^*\vec{\psi}_1) & \cdots & \mathrm{Re}\left[\vec{\psi}_1^*\vec{\psi}_d\right] \\ \vdots & \vdots & \ddots & \vdots \\ \mathrm{Re}\left[\vec{\psi}_d^*\vec{\chi}\right] & \mathrm{Re}\left[\vec{\psi}_d^*\vec{\psi}_1\right] & \cdots & (\vec{\psi}_d^*\vec{\psi}_d) \end{bmatrix}^{-1} \quad (27)$$

In these special cases, the constants in (24) satisfy

$$\begin{aligned} b_{1i} &= \frac{1}{2}\frac{[n!]^2}{[\phi'(q_i)]^2}\alpha_{11}\left(\{\mathrm{Re}\left[\rho\right]\}^{-1}\right)_{ii} \\ b_{ji} &= \frac{1}{2}\alpha_{jj}\left(\{\mathrm{Re}\left[\rho\right]\}^{-1}\right)_{ii} \end{aligned} \quad (28)$$

where ρ denotes the matrix of signal correlation coefficients

$$\rho \triangleq P_D^{-1/2} P P_D^{-1/2} \quad (29)$$

$$P_D \triangleq \mathrm{Diag.}\left[(P)_{11}, (P)_{22}, \cdots (P)_{nn}\right] \quad (30)$$

If Condition III is satisfied, then matrix K is block diagonal and

$$\alpha_{11} = \frac{1}{\|\vec{\chi}\|^2}\ , \quad \alpha_{jj} = \frac{1}{\|\vec{\psi}_j\|^2}\ , \quad \alpha_{kl} = 0 \quad (31)$$

$j = 2 \cdots d$, $k \neq l$. Then the CR bound expressions (24) can be further simplified by referencing the MUSIC null spectrum, as noted in [3] for 1-D scenarios. Specifically (24) takes the remarkably simple form

$$\mathrm{Var}\left\{\hat{\omega}_{ji}\right\} \geq \frac{\left(\{\mathrm{Re}[\rho]\}^{-1}\right)_{ii}}{N \cdot \mathrm{ASNR}_i \cdot D_{jj}^{(2)}(\vec{\omega}_i)}[1 + \mathcal{O}(\delta\omega)] \quad (32)$$

for $i = 1 \cdots n$, $j = 1 \cdots d$, where ASNR_i denotes the array-signal-to-noise ratio for the i^{th} emitter defined as

$$\mathrm{ASNR}_i \triangleq \mathrm{SNR}_i \cdot \|\vec{a}(\vec{\omega}_i)\|^2 \quad (33)$$

and $D_{jj}^{(2)}(\vec{\omega})$ is the second partial derivative along the j^{th} coordinate of the multi-dimensional MUSIC null spectrum

$$D(\vec{\omega}) \triangleq \frac{\vec{a}^*(\vec{\omega})[I - A(A^*A)^{-1}A^*]\vec{a}(\vec{\omega})}{\|\vec{a}(\vec{\omega})\|^2} \quad (34)$$

6. GENERAL EMITTER CONFIGURATIONS

We also have obtained asymptotic expressions for B_C as $\delta\omega \to 0$ for more general emitter configurations [4]. The most striking feature of these results is that B_C increases much less rapidly as $\delta\omega \to 0$ for such emitter configurations than for the co-linear configuration. For example, we have shown for 2-D problems that

$$\begin{aligned} &\mathrm{Var}\left\{\hat{\omega}_{ji}\right\} \propto 1/\delta\omega^2 \quad \text{(3 emitters not constrained to a line)} \\ &\mathrm{Var}\left\{\hat{\omega}_{ji}\right\} \propto 1/\delta\omega^4 \quad \text{(6 emitters not constrained to a conic section)} \end{aligned} \quad (35)$$

By contrast, the corresponding worst-case dependencies for co-linear emitters are $1/\delta\omega^4$ and $1/\delta\omega^{10}$ (See (24)). Thus in multi-D problems the co-linear configuration is an extremely unfavorable one with regard to estimating directional parameters.

7. NUMERICAL EXAMPLES

Example 1: To illustrate the results, asymptotic and exact CR bounds were compared for 2-D direction estimates of far-field emitters located near broadside of a 13 element planar array of omni-directional sensors. 12 of the sensors were uniformly distributed around a circle with unit wavelength spacing between adjacent sensors, and 1 sensor was at the circle center. The array satisfies the Condition II of Section 5.1. Figure 1 shows the values of CR bounds for parameter estimates along the x and y axes for a scenario with two correlated emitters. One of the emitters is exactly at array broadside. The x-axis was selected to coincide with the straight line defined by the two emitters; the y-axis was selected to be the orthogonal axis. The coordinate origin was selected such that $\vec{\omega}_0 = (0, 0)$ was at array broadside. The x-axis formed a 10° angle with the line through the two nearest sensors on the array perimeter and the sensor array center. The emitter correlation coefficient was $\rho_{12} = 0.4 + 0.6i$, where $i = \sqrt{-1}$. The solid curves depict the exact CR bounds; the dashed lines depict the asymptotic behavior predicted by Eqs (24), (28) and (31). Clearly the simplified asymptotic expressions capture the essence of the bounds for emitter separations less than one beamwidth.

Example 2: Exact and asymptotic bounds also were calculated for one of three far-field emitters observed by the sensor array of Example 1. The emitter correlation matrix was

$$\rho = \begin{bmatrix} 1 & \rho_{12} & \cdots & \rho_{12}^{n-1} \\ \rho_{12}^* & 1 & \rho_{12} & \vdots \\ \vdots & \ddots & \ddots & \ddots \\ (\rho_{12}^{n-1})^* & \cdots & \rho_{12}^* & 1 \end{bmatrix} \quad (36)$$

with $\rho_{12} = 0.4 + 0.6i$ and $n = 3$. The bounds for emitters in a triangular distribution (emitter directions are $\vec{\omega}_1 = (\delta\omega/3, 0)$, $\vec{\omega}_2 = (0, 2\delta\omega/3)$, $\vec{\omega}_3 = (0, -\delta\omega/3)$) are compared with the bounds for emitters co-linear with the x-axis ($\vec{\omega}_1 = (0,0)$, $\vec{\omega}_2 = (\delta\omega/3, 0)$, $\vec{\omega}_3 = (\delta\omega, 0)$). Figure 2 presents the results. The graph abcissa measures the minimum separation between $\vec{\omega}_1$ and $\vec{\omega}_2 \cdots \vec{\omega}_n$ in array beamwidths. Once again the asymptotic expressions (dashed lines) closely approximate the exact CR bounds (solid curves) for $\overline{\delta\omega} = \delta\omega \cdot \min_{i \neq 1} \|\vec{q}_1 - \vec{q}_i\|$/beamwidth < 1. Also note that the bound for the linear array increases much more rapidly than that for the triangular array as $\delta\omega \to 0$ in agreement with the discussion of Section 6.

Example 3: To further illustrate the results, exact and asymptotic bounds were calculated for two six-emitter configurations observed by the array of Example 1. The correlation matrix ρ is as in (36) with $n = 6$. The bounds for an emitter distribution that satisfies (35) ($\vec{\omega}_1 = (-\eta, -\eta)$, $\vec{\omega}_2 = (-\eta, 0)$, $\vec{\omega}_3 = (0,0)$,$\vec{\omega}_4 = (0, \eta)$, $\vec{\omega}_5 = (\eta, -\eta)$, $\vec{\omega}_6 = (\eta, 0)$, with $\eta = \delta\omega/\sqrt{5}$) are compared with the bounds for emitters co-linear with the x-axis ($\vec{\omega}_1 = (0,0)$, $\vec{\omega}_2 = (\delta\omega/5, 0)$, $\vec{\omega}_3 = (\delta\omega/3, 0)$, $\vec{\omega}_4 = (2\delta\omega/3, 0)$, $\vec{\omega}_5 = (4\delta\omega/5, 0)$, $\vec{\omega}_6 = (\delta\omega, 0)$). Figure 3 presents the results for the emitter at $\vec{\omega}_1$. Once again, the results are in accordance with our analyses.

8. CONCLUSIONS

The main results of this paper are characterizations of the dependence of the CR variance bound on emitter spacing $\delta\omega$ for small $\delta\omega$ and selected emitter geometries. Simple analytic expressions were derived for special case co-linear emitter scenarios and were cited for other scenarios. It was shown via analysis and simulations that the CR bound is typically much larger as $\delta\omega \to 0$ for co-linear emitters than for general emitter distributions. Thus the results show that *degeneracies are present in multi-D parameter estimation scenarios that are not present in 1-D scenarios.* Specifically emitter resolution and direction estimation can be expected to be much more challenging for some emitter configuration than for others. The case of co-linear emitters appears to be a particularly stressful one.

REFERENCES

[1] P. Stoica, A. Nehorai, "MUSIC, Maximum Likelihood, and Cramer-Rao Bound", *IEEE Trans. ASSP*, Vol. 37, No. 5, May 1989.

[2] S.F. Yau, Y. Bresler, "Worst-Case Cramer-Rao Bound for Parametric Estimation of Superimposed Signals", *Fifth ASSP Workshop on Spect. Est. and Mod.*, pp 187-191, Oct. 1990.

[3] H. Lee, "The Cramer-Rao Bound on Frequency Estimates of Signals Closely Spaced in Frequency (Conditional Signal Model)", *To appear in IEEE Trans. SP.*

[4] J. Jachner, "High-Resolution Direction Finding in Multi-Dimensional Scenarios", *To be submitted as Ph.D. Thesis*, MIT.

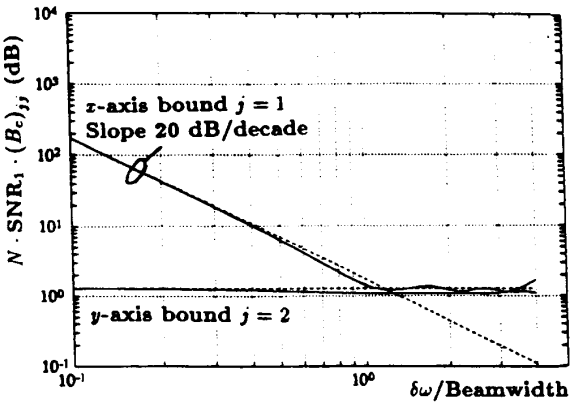

Fig. 1: Exact '–' and Asymptotic '- -' CR Bounds; 2 Correlated Signals in 2-D.

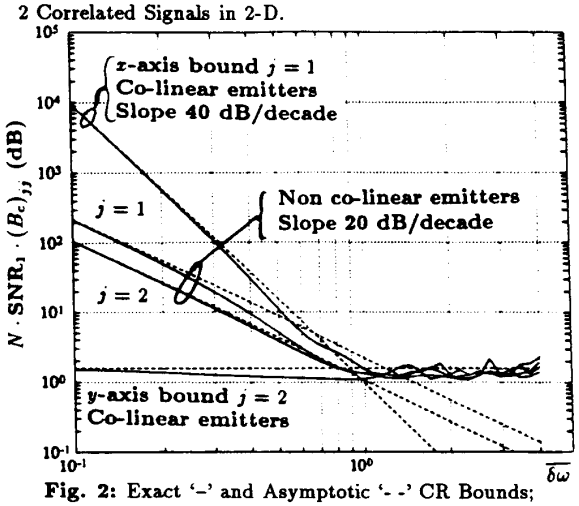

Fig. 2: Exact '–' and Asymptotic '- -' CR Bounds; 3 Correlated Signals in 2-D.

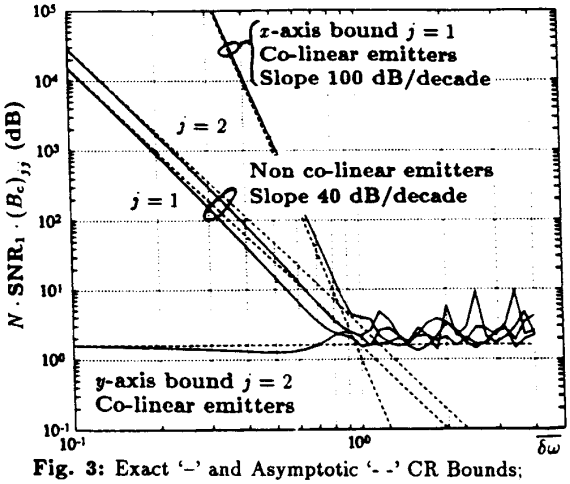

Fig. 3: Exact '–' and Asymptotic '- -' CR Bounds; 6 Correlated Signals in 2-D.